EUROPEAN COMMISSION
DIRECTORATE-GENERAL
Joint Research Centre

Institute for Environment and Sustainability

Medium Resolution Imaging Spectrometer (MERIS)

An optimized FAPAR Algorithm Theoretical Basis Document

Nadine Gobron, Ophélie Aussedat, Bernard Pinty
Malcolm Taberner & Michel Verstraete

Institute for Environment and Sustainability
Joint Research Centre, TP 440
I–21020 Ispra (VA), Italy

| Revision 3.0, November 25, 2004

| **JRC Publication No. EUR 21386 EN**

Contents

List of Figures

List of Tables

1 Introduction

1.1 Purpose

This Algorithm Theoretical Basis Document (ATBD) describes an algorithm used to retrieve information on the nature and properties of vegetated terrestrial surfaces from an analysis of Level 1B data generated by the Medium Resolution Imaging Spectrometer (MERIS) on board of the ENVISAT platform of the European Space Agency (ESA).

The algorithm takes the form of a spectral index, *i.e.*, a set of formulae which transform calibrated spectral directional reflectances into a single numerical value. These formulae are designed to extract some information of interest from the measurements. The index described in this ATBD has been optimized to assess the presence on the ground of healthy live green vegetation. The optimization procedure has been constrained to provide an estimate of the Fraction of Absorbed Photosynthetically Active Radiation (FAPAR) in the plant canopy, although the index is expected to be used in a wide range of applications.

This algorithm delivers, in addition to the FAPAR product, the so-called rectified reflectance values in the red and near-infrared spectral bands. These are virtual reflectances largely decontaminated from atmospheric and angular effects which are still depending on the sensor and platform orbital specifications.

This document identifies the sources of input data, outlines the physical principles and mathematical background justifying this approach, describes the proposed algorithm, and lists the assumptions and limitations of this technique.

Polynomials coefficients values are updated and supersede those given in previous versions of ATBD.

1.2 Algorithm identification

The algorithm described below is called the MERIS Vegetation Index (MGVI). It is suitable for any surface applications requiring the monitoring of the state of the land surface.

1.3 Scope

This document outlines the algorithm which is recommended to generate both a FAPAR product, *i.e.*, the MGVI and the rectified red and near-infrared reflectance values.

1.4 Revision history

The previous version of this document, revision 2.0, was dated January, 22, 2002.

The current version, version 3.0, includes the developments presented in Gobron et al. (2002) and supersedes all previous versions.

1.5 Other relevant documents

Other references to technical reports, ATBDs and additional information about MERIS can be found at the following address:
`http://envisat.estec.esa.nl/Satellite/instrument/MERIS/`. A series of relevant reports and articles are included in the bibliography list of this ATBD.

The associated IDL and C $^{++}$ routines implementing this algorithm are described in Taberner et al. (2002).

A package for the BEAM software is available and can be downloaded from the following ftp anonymous web. site: `ftp-gvm.jrc.it` in the directory `/gobrona/beam/mgvi/`

A time compositing procedure suitable for a number of surface applications requiring good geographical coverage is described in Pinty et al. (2002).

Validation exercices are on going since the launch on ENVISAT (see Gobron et al. (2002), Gobron et al. (2003) and Gobron et al. (2003))

2 Algorithm overview

2.1 Objectives of surface retrievals

The bulk of the solar radiation available to the Earth system is absorbed at or near the oceanic and continental surface. This energy is ultimately released to the atmosphere through the fluxes of infrared radiation, as well as sensible and latent heat. The phytosphere, which itself accounts for most of the biomass, affects these exchanges through a surface of contact (leaves) with the atmosphere estimated to be larger than the surface of the entire planet.

The state and evolution of terrestrial vegetation is characterized by a large number of physical, biochemical and physiological variables. Few of these are directly observable from space, but they jointly determine the Fraction of Absorbed Photosynthetically Active Radiation (FAPAR) which acts as an integrated indicator of the status and health of the plant canopy, and can reasonably be expected to be retrieved by remote sensing techniques. FAPAR plays a critical role in the biospheric path of the global carbon cycle and in the determination of the primary productivity of the phystosphere.

The state and evolution of the terrestrial vegetation cover thus concern a large number of users through such applications as agriculture, forestry, environmental monitoring, etc. Since plant canopies significantly affect the spectral and directional reflectance of solar radiation, it is expected that the analysis of repeated observations of these reflectances may lead to a better understanding of the fundamental processes controlling the biosphere, which, in turn, will support the definition of sustainable policies of environmental exploitation, and the control of the effectiveness of any adopted rules and regulations.

The overall scientific objective of the MERIS Global Vegetation Index is to exploit the spectral reflectance measurements acquired by this instrument to provide users with reliable qualitative and quantitative information on the state of the plant cover over terrestrial areas. Specifically, the index value is meant to be easily interpreted in terms of FAPAR values.

The design of the MERIS Global Vegetation Index requires, in a first step, the estimate of the so-called rectified reflectances at the red and near-infrared wavelengths in order to minimize atmospheric and angular perturbations. These intermediary land surface products should prove useful for documenting the state of the land surfaces and also assessing the spatio-temporal variations in land cover type. Specifically, these rectified reflectances correspond to the amplitude parameter of the BRF entering the Rahman, Pinty, Verstraete (RPV) parametric model (Rahman et al. 1993). These are virtual, *i.e.*, not directly measurable in the field, spectral reflectances which are, at best, decontaminated from atmospheric and angular effects.

2.2 Instrument characteristics

The MERIS instrument has been described in a number of publications, such as MERIS Scientific Advisory Group (1995) and Rast et al. (1999). For the purpose of this document, it is sufficient to recall that MERIS is a programmable push-broom instrument acquiring multispectral measurements between 390 and 1040 nm, at a minimum usable resolution of 5 nm. Fifteen bands of programmable location and width can be downloaded simultaneously at the full resolution of approximately 300 m, at least for limited regions. Global coverage at a spatial resolution of 1.2 km will be operationally available on a daily basis. MERIS is not designed to acquire simultaneous measurements over any particular site under more than one geometry of illumination and observation, however, orbital constraints and instrumental specifications will inevitably result in different such geometries from pixel to pixel within a single image and for any given location between overpasses on consecutive days. The proposed algorithm will thus focus on the exploitation of the spectral variability of the data, keeping in mind the possible perturbing effects that may result from variations in geometry within and between successive images.

2.3 Retrieval strategy

Monitoring the state and evolution of the vegetation cover is traditionally done with the Normalized Difference Vegetation Index (NDVI). Many applications have relied on this index for numerous purposes over the last 20 years or so. It has long been known, however, that this index is quite sensitive to perturbing factors such as changes in soil colour, atmospheric effects, or to the particular geometry of illumination and observation at the time of data acquisition (*e.g.*, Huete 1988; Kaufman and Tanré 1992). Other investigations have shown, on the basis of model simulations, the extent of these perturbations (*e.g.*, Pinty et al. 1993; Goel and Qin 1994; Leprieur et al. 1994). New and better performing indices such as the Global Environment Monitoring Index (GEMI) have been proposed for the NOAA-AVHRR instrument. GEMI is a non-linear spectral index designed to simultaneously minimize the soil and the atmospheric effects (Pinty and Verstraete 1992) while retaining a high sensitivity of vegetation properties.

The specific objective of this ATBD is to describe a spectral index suitable to estimate FAPAR, optimized for the MERIS instrument. The design criteria will be

1. to provide a high sensitivity to the Fraction of Absorbed Photosynthetically Active Radiation (FAPAR) when a vegetated area is detected,
2. to maintain a low sensitivity to soil and atmospheric conditions whenever vegetation is detected,
3. to exploit the multi-band specificity of the MERIS sensor,
4. to be independent of the geometry of illumination and observation, and
5. to offer excellent discrimination capabilities, *i.e.*, the opportunity to distinguish various target types.

3 Algorithm description

3.1 Physics of the problem

The general theory behind the design of optimal spectral indices has been described in Verstraete and Pinty (1996), and its specific application to upcoming instruments has been addressed in Govaerts et al. (1999), Gobron et al. (1999) and Gobron et al. (2000). The most recent implementation of the algorithm assumes that, 1) the FAPAR can be used to quantify the presence of vegetation and, 2) radiation transfer model simulations can be used to define appropriate scenarios over different representative land surfaces.

The bulk of the information on the presence of vegetation is contained *a priori* in the red and the near-infrared spectral bands, typically at wavelengths such as 681 and 865 nm. Addressing the atmospheric problem consists in converting Top Of Atmosphere (TOA) Bidirectional Reflectance Factors (BRFs) into Top Of Canopy (TOC) BRFs.

Two classes of atmospheric radiative processes affect the measurements made by space-borne satellites: absorption and scattering. Absorption of radiation by specific gases can be largely avoided by carefully choosing the spectral location of narrow bands. Further corrections can be implemented, if needed, by estimating the amount of these gases from other spectral bands. The effect of scattering cannot be avoided, and both molecular and aerosol scattering are strongly dependent on the wavelength of radiation. Hence, measurements in the blue region of the solar spectrum will provide values much more sensitive to atmospheric scattering than at longer wavelengths. In this approach, the characterization of plant canopies over fully or partially vegetated pixels currently relies on the analysis of data in 3 MERIS spectral bands, namely 442, 681, and 865 nm.

A LookUp Table (LUT) of bidirectional reflectance factors representing the MERIS-like data has been created using the physically-based semidiscrete model of Gobron et al. (1997) to represent the spectral and directional reflectance of horizontally homogeneous plant canopies, as well as to compute the values of FAPAR in each of them. The soil data required to specify the lower boundary condition in this model were taken from Price (1995). The spectral values for the leaf reflectance and transmittance were simulated using the model from Jacquemoud and Baret (1990). The 6S atmospheric model of Vermote et al. (1997) has been used to represent the atmospheric absorption and scattering effects on the measured reflectances. The FAPAR values are computed using the closure of the energy balance inside the plant canopy in the spectral range 400 to 700 nm. The various geophysical scenarios performed to simulate the radiance fields are summarized in Table 1 and the geometrical conditions of illumination and observation are given in Table 2. The sampling of the vegetation parameters and angular values were chosen to cover a wide range of environmental conditions. These simulations constitute the basic information used to optimize the vegetation index. The sampling selected to generate the LUT has been chosen so as to generate a robust global vegetation index.

Once this LUT has been created, the design of an optimal spectral index consists in defining the mathematical combination of spectral bands which will best account for the variations of the variable of interest (here, FAPAR) on the basis of (simulated) measurements, while minimizing the effect of perturbing factors such as atmospheric or angular effects. This process is described in the next section.

Table 1: Geophysical scenarios used to simulate the radiance fields.

Medium	**Variable**	**Meaning**	**Range of values**
Atmosphere model (Vermote *et al.*, 1997)	τ_s	Aerosol opt. thickness	0.05, 0.3 and 0.8
Vegetation model (Gobron *et al.*, 1997)	LAI	Leaf Area Index	0, 0.5, 1, 2, 3, 4, and 5
	H_c	Height of Canopy	0.5 m and 2 m
	d_ℓ	Equivalent diameter of single leaf	0.01 m and 0.05 m
	LAD	Leaf Angle Distribution	Erectophile, Planophile
Soil data base (Price, 1995)	r_s	Soil reflectance	5 soil spectra, from dark to bright

Table 2: Illumination and observation geometries used to simulate the radiance fields.

Variable	**Angle**	**Values**
θ_0	Solar zenith angle	20° and 50°
θ_v	Sensor zenith angle	0°, 25°and 40°
phi	Sun-Sensor relative azimuth	0°, 90° and 180°

3.2 Mathematical description of the algorithm

The proposed algorithm to compute MGVI, the FAPAR value, is organized around three main consecutive steps.

1. As mentioned previously, because of the actual sampling strategy implemented by the MERIS instrument in the angular domain, it is not possible to retrieve the anisotropy of the radiance field. A parametric anisotropic function is implemented to account for variations in the signal due to changes in the geometrical conditions. The bidirectional reflectance model of Rahman et al. (1993) (RPV) is assumed to be appropriate for this task:

$$\rho_i(\theta_0, \theta_v, \phi) = \rho_{i0}\, F(\theta_0, \theta_v, \phi; k_i, \Theta_i^{hg}, \rho_{ic}) \tag{1}$$

where F characterizes the anisotropy of the medium in terms of three unknown parameters, namely k_i, Θ_i^{hg} and ρ_{ic} which depend exclusively on the intrinsic properties of the type of geophysical system for a given spectral band i. The function $F(\Omega; k_i, \Theta_i^{hg}, \rho_{ic})$ with $\Omega = (\theta_0, \theta_v, \phi)$ is given by:

$$F(\Omega; k_i, \Theta_i^{hg}, \rho_{ic}) = f_1(\theta_0, \theta_v, k_i)\, f_2(\Omega, \Theta_i^{hg})\, f_3(\Omega, \rho_{ic}) \tag{2}$$

where

$$f_1(\theta_0, \theta_v, k_i) \;=\; \frac{(\cos\theta_0\, \cos\theta_v)^{k_i - 1}}{(\cos\theta_0 + \cos\theta_v)^{1-k_i}} \tag{3}$$

$$f_2(\Omega, \Theta_i^{hg}) = \frac{1 - {\Theta_i^{hg}}^2}{\left(1 + 2\,\Theta_i^{hg}\,\cos g + {\Theta_i^{hg}}^2\right)^{3/2}} \quad (4)$$

$$f_3(\Omega, \rho_{ic}) = 1 + \frac{1 - \rho_{ic}}{1 + G} \quad (5)$$

with

$$G = \left(\tan^2\theta_0 + \tan^2\theta_v - 2\,\tan\theta_0\,\tan\theta_v\,\cos\phi\right)^{1/2} \quad (6)$$

$$\cos g = \cos\theta_0\,\cos\theta_v + \sin\theta_0\,\sin\theta_v\cos\phi \quad (7)$$

The characterization of a geophysical system with the RPV model thus requires the estimation of four parameter values, namely ρ_{i0}, k_i, Θ_i^{hg} and, ρ_{ic} which are independent of the geometry of illumination and observation Ω.

The parameters intervening in function F are optimized separately in the three bands using the simulated BRFs emerging at the top of atmosphere.

2. The information contained in the spectral band centered at 442 nm is combined with that in the bands centered at 681 nm and 865 nm traditionally used to monitor vegetation, in order to generate "rectified bands" at these latter two wavelengths. The "rectification" is done in such a way as to minimize the difference between those rectified bands and the spectral reflectances that would have been measured at the top of the canopy under identical geometrical conditions but in the absence of the atmosphere.

3. The vegetation spectral index, MGVI, is generated on the basis of these "rectified bands".

The proposed algorithm assumes that ratios of polynomials are appropriate to generate both the "rectified bands" with the following generic formula:

$$g_n(B_1, B_2) = \frac{l_{n,1}(B_1 + l_{n,2})^2 + l_{n,3}(B_2 + l_{n,4})^2 + l_{n,5}B_1B_2}{l_{n,6}(B_1 + l_{n,7})^2 + l_{n,8}(B_2 + l_{n,9})^2 + l_{n,10}B_1B_2 + l_{n,11}} \quad (8)$$

where B_1 and B_2 are the spectral bands at the appropriate step. The MGVI formula itself is given by the following formulae:

$$g_0(B_1, B_2) = \frac{l_{0,1}\,B_2 - l_{0,2}\,B_1 - l_{0,3}}{(l_{0,4} - B_1)^2 + (l_{0,5} - B_2)^2 + l_{0,6}} \quad (9)$$

$$\mathrm{MGVI} = g_0(\rho_{R681}, \rho_{R865}) \quad (10)$$

where ρ_{R681} and ρ_{R865} are the rectified reflectance values in the red and near-infrared bands described above. These, in turn, are estimated with

$$\rho_{R681} = g_1(\tilde{\rho}_{442}, \tilde{\rho}_{685}) \quad (11)$$

$$\rho_{R865} = g_2(\tilde{\rho}_{442}, \tilde{\rho}_{865}) \quad (12)$$

where

$$\tilde{\rho}_i = \frac{\rho_i^*(\theta_0, \theta_v, \phi)}{F(\theta_0, \theta_v, \phi; k_i, \Theta_i^{hg}, \rho_{ic})} \tag{13}$$

and where ρ_i^* denotes the (simulated) top of atmosphere bidirectional reflectance factor in band i, while $\tilde{\rho}_i$ is the bidirectional reflectance factor normalized by the anisotropic function F. An optimization procedure is applied to retrieve successively the optimal values of the coefficients intervening in the three steps mentioned above, namely k_i, Θ_i^{hg} and ρ_{ic}, and $l_{n,j}$ for the polynomials g_n, both for the rectified bands and for the final index itself.

1. In the first step, it is assumed that the anisotropic shapes of the BRFs simulated at the top of the atmosphere may change with the spectral wavelength of interest, but do not depend on the geophysical systems specified to generate the BRFs. Accordingly, for a given spectral band, the three parameters of the anisotropic function F are forced to be constant over the entire set of geophysical scenarios considered. In practice, this condition is achieved by minimizing the following cost functions:

$$\delta_i^2 = \sum_{\zeta,\Omega} \left[\left(\frac{\rho_i^*(\Omega)}{F(\Omega; k_i, \Theta_i^{hg}, \rho_{ic})} \right) - \tilde{\rho}_i \right]^2 \rightarrow 0 \tag{14}$$

   where ζ represents the geophysical domain and Ω the angular domain over which the optimization is sought.

   Since $\tilde{\rho}_i$ is assumed to be constant in the RPV model for each individual geophysical system taken separately, we can estimate the mean value of the BRFs over the Ω space for every geophysical system:

$$\frac{1}{N_{obs}} \sum_{\Omega} \rho_i^*(\Omega_j) = \frac{1}{N_{obs}} \sum_{\Omega} \tilde{\rho}_i \times F(\Omega_j; k_i, \Theta_i^{hg}, \rho_{ic}) \tag{15}$$

$$= \tilde{\rho}_i \frac{1}{N_{obs}} \sum_{\Omega} F(\Omega_j; k_i, \Theta_i^{hg}, \rho_{ic}) \tag{16}$$

   where N_{obs} is the total number of angular situations. The model coefficient $\tilde{\rho}_i$ is thus approximated for each geophysical system as

$$\tilde{\rho}_i = \frac{1}{N_{obs}} \sum_{\Omega} \rho_i^*(\Omega_j) \Big/ \frac{1}{N_{obs}} \sum_{\Omega} F(\Omega_j; k_i, \Theta_i^{hg}, \rho_{ic}) \tag{17}$$

   The cost function is rewritten as follows:

$$\delta_i^2 = \sum_{\zeta} \left[\frac{\rho_i^*(\Omega)}{F(\Omega; k_i, \Theta_i^{hg}, \rho_{ic})} \frac{1}{N_{obs}} \sum_{\Omega} F(\Omega_j; k_i, \Theta_i^{hg}, \rho_{ic}) - \frac{1}{N_{obs}} \sum_{\Omega} \rho_i^*(\Omega_j) \right]^2 \rightarrow 0 \tag{18}$$

2. To satisfy the various requirements described above, the optimization procedure is applied in the 681 nm and 865 nm bands separately, to derive the coefficients of g_1 and g_2. This is achieved by minimizing the following cost functions:

$$\delta_{g_i}^2 = \sum_{\zeta} \left[g_i(\tilde{\rho}_{442}, \tilde{\rho}_i) - \tilde{\rho}_i^{TOC} \right]^2 \rightarrow 0. \tag{19}$$

where

$$\tilde{\rho}_i^{TOC} = \frac{\rho_i^{TOC}(\Omega)}{F(\Omega, k_i^{TOC}, \Theta_i^{hg,TOC}, \rho_{ic}^{TOC})} \tag{20}$$

for which the anisotropic parameters, namely $k_i^{TOC}, \Theta_i^{hg,TOC}, \rho_{ic}^{TOC}$, were previously optimized at the top of canopy level.

3. Following the rectification of the BRFs in the previous step, the coefficients of g_0 are evaluated by minimizing the following cost function:

$$\delta_{g_0}^2 = \sum_{\zeta} [g_0(\rho_{R681}, \rho_{R865}) - \text{FAPAR}]^2 \rightarrow 0. \tag{21}$$

In other words, the MGVI is forced to take on values as close as possible to the FAPAR associated with the specified plant canopy scenarios. The simulated top-of-atmosphere spectral and directional reflectances generated by the coupled model have been exploited with an extended version of the FACOSI tool (Govaerts et al. 1999) to adjust the MGVI on the basis of the given set of equations. The numerical results are summarized in Tables 3 to 6.

Figures (1) and (2) illustrate the impact of the "rectification" procedure, which combines TOA reflectances in the 442 nm band with TOA reflectances in the 681 nm and 865 nm bands, respectively. The left panels on these figures show the relationships between the spectral BRFs TOC normalized by the anisotropic function F, and BRFs TOA for all geophysical and angular scenarios described in Table 1. The scattering of the points is caused by changes in the atmospheric conditions and by the relative geometry of illumination and observation. The right panels show the effect of the "rectification" process, which reduces this dispersion. A perfect "rectification" would collapse all points on the 1:1 line for each of the surface types considered. It can be seen that this process is particularly efficient over dense vegetation, and that it reduces the systematic bias due to atmospheric effects on BRFs in both bands.

Figure (3) provides information on the performance of MGVI. The right panel shows the isolines of the MGVI in the spectral space of the rectified bands at 681 nm and 865 nm. It can be seen that the MGVI varies between 0 and 1 over partially and fully vegetated surfaces and takes negative values out of the spectral domain of interest. The left panel of the same figure shows that the MGVI is close to the FAPAR with a root mean square deviation equal to 0.07. Most of the remaining variability between FAPAR and MGVI is probably caused by the various conditions that were considered in the geophysical scenarios (see Table 1). In fact, this variability results from conflicting requirements on the insensitivity of the MGVI to soil, atmospheric and geometrical effects in the MERIS spectral bands.

4 Error budget estimates

Since the MGVI has been optimized to provide a high sensitivity to FAPAR, a measurable biophysical variable, its capacity to detect the presence of green vegetation can be objectively assessed. For the particular geophysical scenarios in Table 1 and angular sampling given in Table 2, the root mean square deviation value of the fit between these two quantities is 0.05. Following the method proposed by Leprieur et al. (1994), the performance

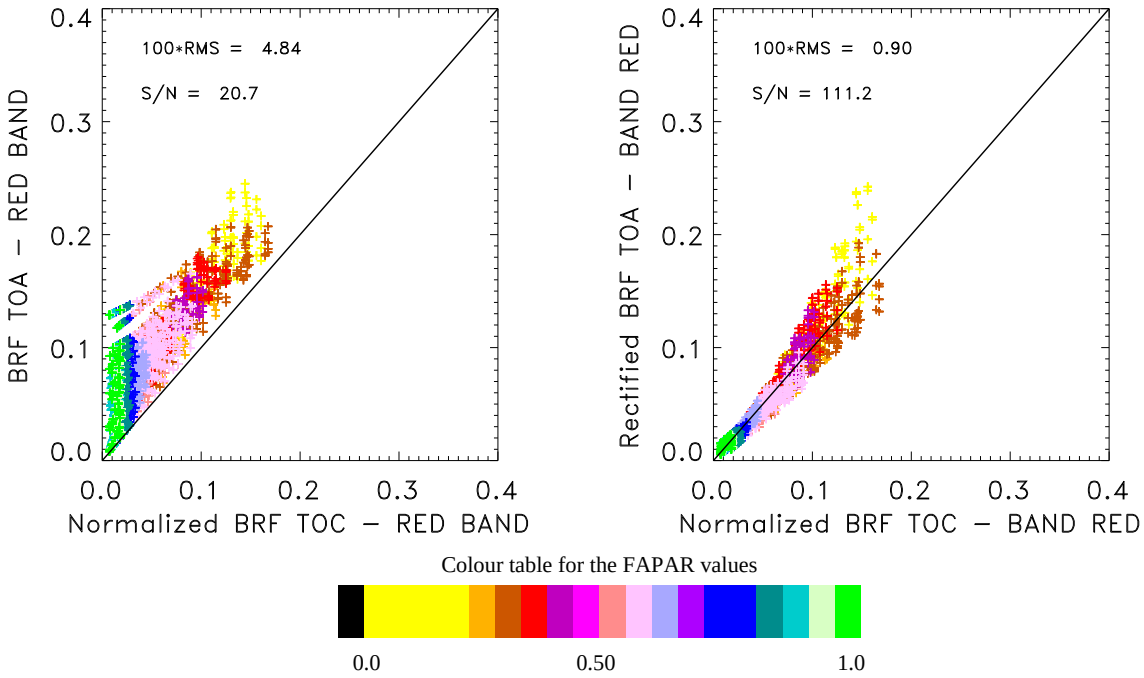

Figure 1: **NEW** Left panel: relationship between the BRFs TOC normalized by the anisotropic function F, and BRFs TOA, for all conditions given in Table 1, in the 681 nm band. Right panel: relationship between the "rectified" reflectances and the corresponding BRFs TOC normalized by the anisotropic function F. The various colours represent different values of FAPAR for the plant canopies described in Table 1.

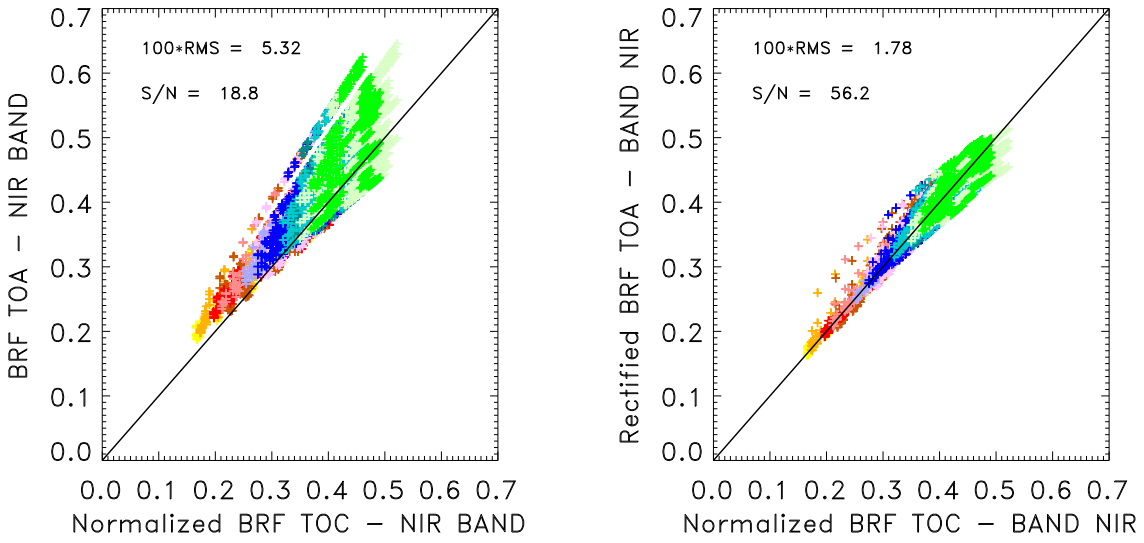

Figure 2: **NEW** Same as Figure (1) except for the 865 nm band.

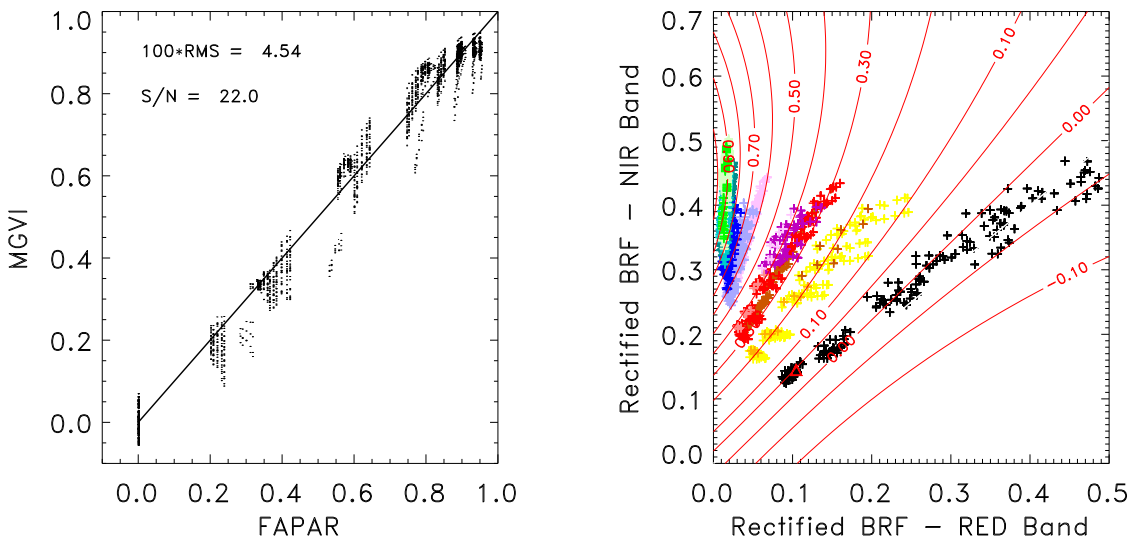

Figure 3: **NEW** The right panel shows the isolines of MGVI in the Rectified (681 nm, 865 nm) spectral space together with the simulated radiances at the top of the atmosphere (see Table 1). The left panel shows the relationship between the index and the FAPAR values.

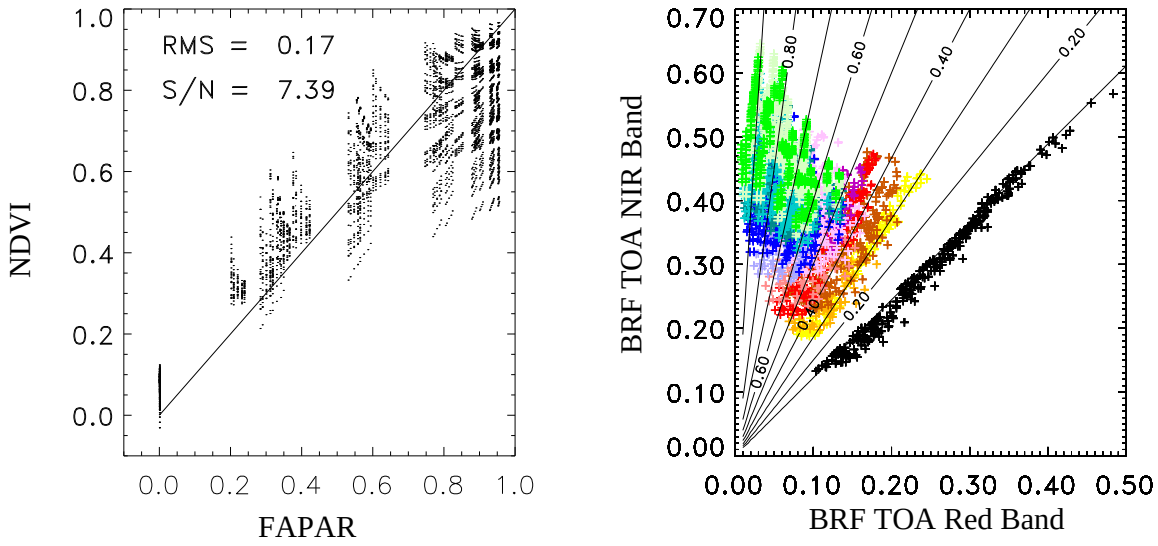

Figure 4: The right panel shows the isolines of NDVI in the (681 nm, 865 nm) spectral space together with the simulated radiances at the top of the atmosphere (see Table 1). The left panel shows the relationship between the index and the FAPAR values.

Table 3: **NEW** Values of the parameters for the anisotropic function F.

band	**Parameter values**		
	ρ_{ic}	k_i	Θ_i^{hg}
442 nm	0.24012	0.56192	−0.04203
681 nm	−0.46273	0.70879	0.037
865 nm	0.63841	0.86523	−0.00123

Table 4: **NEW** Coefficients for the polynomial g_1.

$l_{1,1}$	$l_{1,2}$	$l_{1,3}$	$l_{1,4}$	$l_{1,5}$	
−9.2615	−0.029011	3.2545	0.055845	9.8268	
$l_{1,6}$	$l_{1,7}$	$l_{1,8}$	$l_{1,9}$	$l_{1,10}$	$l_{1,11}$
0	0	0	0	0	1.0

Table 5: **NEW** Coefficients for the polynomial g_2.

$l_{2,1}$	$l_{2,2}$	$l_{2,3}$	$l_{2,4}$	$l_{2,5}$	
−0.47131	−0.21018	−0.045159	0.076505	−0.80707	
$l_{2,6}$	$l_{2,7}$	$l_{2,8}$	$l_{2,9}$	$l_{2,10}$	$l_{2,11}$
0.048362	−1.2471	−0.54507	−0.47602	−1.1027	0.0

Table 6: **NEW** Coefficients for the polynomial g_0.

$l_{0,1}$	$l_{0,2}$	$l_{0,3}$	$l_{0,4}$	$l_{0,5}$	$l_{0,6}$
0.255	0.306	−0.0045	−0.32	0.32	−0.005

of MGVI can be evaluated with the help of a signal to noise ratio. In the present case, it was found that the signal to noise ratio of the MGVI is equal to **22.00**. By comparison, the widely used Normalized Difference Vegetation Index (NDVI), computed on the basis of bands at 681 nm and 865 nm exhibits a non-linear relationship with respect to FAPAR variations and the corresponding signal to noise ratio is only 7.39 (see Figure 4).

4.1 Practical considerations

4.1.1 Quality control and diagnostics

A simple approach is proposed to associate a label to each pixel of the MERIS data in order to optimize the various steps of the processing to be achieved over water bodies and land surfaces.

Table 7 indicates the tests applied and the associated categories for discriminating the major geophysical systems (also identified with an identification number), namely clouds,

bright surfaces, vegetated surfaces and water bodies. In the data product, the various identification numbers correspond to a set of flag values.

As can be seen from Table 7, the pixel labelling is performed on the basis of an ensemble of thresholds using only the values in the bands centered at 442 nm, 681 nm and 865 nm. For each geophysical category, the ensemble of tests has been established on the basis of knowledge of the multispectral signatures of the geophysical systems. The proposed approach classifies the vast majority of the pixels without requiring any other ancillary information. A more sophisticated labelling scheme could not be reasonably considered given the processing constraints imposed by the computing resources.

4.1.2 Output

The output generated by this algorithm consists in one index value *i.e.*, the FAPAR, for the MGVI, one for the rectified red, and one for the rectified near infrared, one for each of the associated spectral BRF values estimated at the top of the atmosphere. The ouput field also contains the description of the geometry of illumination and observation, and one flag value for each pixel in the data input stream.

The flag value corresponds to the identification (ID) numbers described in section 4.1.1. If the ID value is equal to 0, the value of MGVI is considered valid and the physical range of values lies in between 0 and 1.0.

If the ID number is equal either to 1 ("bad data"), 2 ("cloud, snow and ice") or 3 ("water body and deep shadow"), the value of MGVI has not been computed and the reported value is equal to its error value.

If the ID number is equal to 4 ("bright surface"), the value of MGVI has been set at 0.

If ID number is equal to 5 ("undefined"), the value of MGVI has not been computed and the reported value is set to its error value.

If the ID number is equal to 6, the value of MGVI was less than 0 and the reported value is equal to 0.

If the ID number is equal to 7, the value of MGVI was larger than 1 and the reported value is reset to 1.

5 Assumptions and limitations

5.1 Assumptions

The following assumptions have been made in the design of the MERIS Vegetation Index (MGVI):

1. The spectral reflectances used as input to this algorithm will have been corrected for the seasonally variable distance between the Earth and the Sun.

2. The plane-parallel approximation for radiation transfer has been assumed to be valid in the atmosphere.

3. Plant canopies are assumed to be horizontally homogeneous within the MERIS pixel.

4. All orographic effects have been ignored.

Table 7: Pixel labelling criteria

Identification number (ID)	**Spectral tests**	**Associated categories**
0	$0 < \rho_{442} < 0.3$ and $0 < \rho_{681} < 0.5$ and $0 < \rho_{865} < 0.7$ and $0 < \rho_{442} \leq \rho_{865}$ and $\rho_{865} \geq 1.25\,\rho_{681}$	vegetated surface
1	$\rho_{442} \leq 0$ or $\rho_{681} \leq 0$ or $\rho_{865} \leq 0$	bad data
2	$\rho_{442} \geq 0.3$ or $\rho_{681} \geq 0.5$ or $\rho_{865} \geq 0.7$	cloud, snow and ice
3	$0 < \rho_{442} < 0.3$ and $0 < \rho_{681} < 0.5$ and $0 < \rho_{865} < 0.7$ and $\rho_{442} > \rho_{865}$	water body and deep shadow
4	$0 < \rho_{442} < 0.3$ and $0 < \rho_{681} < 0.5$ and $0 < \rho_{865} < 0.7$ and $0 < \rho_{442} \leq \rho_{865}$ and $1.25\,\rho_{681} > \rho_{865}$	bright surface
5	$\rho_{R681} < 0$ or $\rho_{R865} < 0$	undefined
6	$VI < 0$	no vegetation
7	$VI > 1$	vegetation (out of bounds)

5. Adjacency effects have been ignored.

5.2 Limitations

The following limitations apply to the algorithm described in this version of the document:

1. The retrieval of vegetation characteristics in hilly or mountainous regions may or may not be reliable. If the approach turns out to be unreliable in the presence of significant topographical features, additional tests may have to be implemented to screen out these regions on the basis of appropriate DEM data. This would imply access to the corresponding elevation data sets, to reliably navigated MERIS data, and the presence of an additional orographic flag.

2. The optimization of the MGVI was performed using a set of simulated TOA reflectance values which are expected to represent the most commonly encountered geophysical conditions. Although a wide range of possibilities were investigated, there is no guarantee that the most common geophysical scenarios have been implemented. If this is not the case, this may result in a systematic bias in the relationship between the MGVI and the FAPAR.

6 Algorithm requirements

The implementation of the proposed algorithm to estimate MGVI requires three different types of information, namely, the input data from the MERIS sensor, a set of ancillary data and a set of mathematical functions. The ancillary data are the set of coefficients given in Tables 3 to 6. The mathematical functions are given by equations (2), (8), (9) and (13).

The input data are the BRFs measured by the instrument at 443 nm, 678 nm and 865 nm, together with the geometrical conditions of illumination and observation, namely θ_0, θ_v, ϕ. The sun-sensor relative azimuth, ϕ, is limited to the range [0°, 180°] and the backscatter/hot spot (forwardscatter/specular) direction is defined at 0° (180°).

References

Gobron, N., F. Mélin, B. Pinty, M. Taberner, and M. M. Verstraete (2003). Meris global vegetation index: Evaluation and performance. In *Proceedings of the MERIS User Workshop, Frascati, Italy, 10-14 November*, Volume SP 549, pp. pp 15. European Space Agengy.

Gobron, N., B. Pinty, M. M. Verstraete, and Y. Govaerts (1997). A semi-discrete model for the scattering of light by vegetation. *Journal of Geophysical Research 102*, 9431–9446.

Gobron, N., B. Pinty, M. M. Verstraete, and Y. Govaerts (1999). The MERIS Global Vegetation Index (MGVI): description and preliminary application. *International Journal of Remote Sensing 20*, 1917–1927.

Gobron, N., B. Pinty, M. M. Verstraete, and J.-L. Widlowski (2000). Advanced spectral algorithm and new vegetation indices optimized for up coming sensors: Development, accuracy and applications. *IEEE Transactions on Geoscience and Remote Sensing 38*, 2489–2505.

Gobron, N., M. Taberner, B. Pinty, F. Mélin, M. Verstraete, and J.-L. Widlowski (2002). Meris land algorithm: preliminary results. In *Proceedings of the ENVISAT Validation Workshop*, Volume SP 531, pp. pp. 10. European Space Agengy.

Gobron, N., M. Taberner, B. Pinty, F. Mélin, and M. M. Verstraete (2003). Meris global vegetation index: Evaluation and performance. In *Proceedings of the MERIS and ATSR Calibration and Geophysical Validation (MAVT), Frascati, Italy, 20-23 October, 2003*, Volume SP 541, pp. pp 15. European Space Agengy.

Goel, N. S. and W. Qin (1994). Influences of canopy architecture on relationships between various vegetation indices and LAI and FPAR: A computer simulation. *Remote Sensing Reviews 10*, 309–347.

Govaerts, Y., M. M. Verstraete, B. Pinty, and N. Gobron (1999). Designing optimal spectral indices: a feasibility and proof of concept study. *International Journal of Remote Sensing 20*, 1853–1873.

Huete, A. R. (1988). A soil-adjusted vegetation index (SAVI). *Remote Sensing of Environment 25*, 295–309.

Jacquemoud, S. and F. Baret (1990). PROSPECT: A model of leaf optical properties spectra. *Remote Sensing of Environment 34*, 75–91.

Kaufman, Y. J. and D. Tanré (1992). Atmospherically Resistant Vegetation Index (ARVI) for EOS-MODIS. *IEEE Transactions on Geoscience and Remote Sensing 30*, 261–270.

Leprieur, C., M. M. Verstraete, and B. Pinty (1994). Evaluation of the performance of various vegetation indices to retrieve vegetation cover from AVHRR data. *Remote Sensing Reviews 10*, 265–284.

MERIS Scientific Advisory Group (1995). MERIS: The Medium Resolution Imaging Spectrometer. Technical Report SP–1184, European Space Agency, Noordwijk.

Pinty, B., N. Gobron, F. Mélin, and M. M. Verstraete (2002). A Time Composite Algorithm Theoretical Basis Document. EUR Report No. 20150 EN, Joint Research Centre, Institute for Environment and Sustainability.

Pinty, B., C. Leprieur, and M. M. Verstraete (1993). Towards a quantitative interpretation of vegetation indices. part 1: Biophysical canopy properties and classical indices. *Remote Sensing Reviews 7*, 127–150.

Pinty, B. and M. M. Verstraete (1992). GEMI: A non-linear index to monitor global vegetation from satellites. *Vegetatio 101*, 15–20.

Price, J. C. (1995). Examples of high resolution visible to near-infrared reflectance spectra and a standardized collection for remote sensing studies. *International Journal of Remote Sensing 16*, 993–1000.

Rahman, H., B. Pinty, and M. M. Verstraete (1993). Coupled surface-atmosphere reflectance (CSAR) model. 2. Semiempirical surface model usable with NOAA Ad-

vanced Very High Resolution Radiometer data. *Journal of Geophysical Research 98*, 20,791–20,801.

Rast, M., J.-L. Bézy, and S. Bruzzi (1999). The ESA Medium Resolution Imaging Spectrometer MERIS -a review of the instrument and its mission. *International Journal of Remote Sensing 20*, (1682–1701).

Taberner, M., N. Gobron, F. Mélin, B. Pinty, and M. M. Verstraete (2002). The STARS FAPAR algorithm: A consolidated and generalized software package. EUR Report No. 20145 EN, Joint Research Centre, Institute for Environment and Sustainability.

Vermote, E., D. Tanré, J. L. Deuzé, M. Herman, and J. J. Morcrette (1997). Second simulation of the satellite signal in the solar spectrum: An overview. *IEEE Trans. Geoscience Remote Sensing 35-3*, 675–686.

Verstraete, M. M. and B. Pinty (1996). Designing optimal spectral indices for remote sensing applications. *IEEE Transactions on Geoscience and Remote Sensing 34*, 1254–1265.

ISBN 92-894-8444-6

9 789289 484442